AD_____

Award Number: W81XWH-11-1-0491

TITLE: Role of MicroRNA in Aggressive Prostate Cancer

PRINCIPAL INVESTIGATOR: Hsieh, Jer-Tsong

CONTRACTING ORGANIZATION: University of Texas, Southwestern Medical Center at Dallas
Dallas, TX 75390-9110

REPORT DATE: July 2014

TYPE OF REPORT: Annual

PREPARED FOR: U.S. Army Medical Research and Materiel Command
Fort Detrick, Maryland 21702-5012

REPORT DOCUMENTATION PAGE

Form Approved
OMB No. 0704-0188

1. REPORT DATE	2. REPORT TYPE	3. DATES COVERED
July 2014	Annual	15 June 2013 - 14 June 2014

4. TITLE AND SUBTITLE
Role of MicroRNA in Aggressive Prostate Cancer

5a. CONTRACT NUMBER

5b. GRANT NUMBER
W81XWH-11-1-0491

5c. PROGRAM ELEMENT NUMBER

6. AUTHOR(S)
Jer-Tsong Hsieh
Betty Diamond

E-Mail: jt.hsieh@utsouthwestern.edu

5d. PROJECT NUMBER

5e. TASK NUMBER

5f. WORK UNIT NUMBER

7. PERFORMING ORGANIZATION NAME(S) AND ADDRESS(ES)

University of Texas, Southwestern Medical Center at Dallas

Dallas, TX 75390

8. PERFORMING ORGANIZATION REPORT NUMBER

9. SPONSORING / MONITORING AGENCY NAME(S) AND ADDRESS(ES)
U.S. Army Medical Research and Materiel Command
Fort Detrick, Maryland 21702-5012

10. SPONSOR/MONITOR'S ACRONYM(S)

11. SPONSOR/MONITOR'S REPORT NUMBER(S)

12. DISTRIBUTION / AVAILABILITY STATEMENT
Approved for Public Release; Distribution Unlimited

13. SUPPLEMENTARY NOTES

14. ABSTRACT
The majority of mortality of prostate cancer (PCa) is due to the recurrent metastasized castration resistance PCa. The acquisition of epithelial–to-mesenchymal transition (EMT) in PCa signifies the initial process of cancer metastasis. Our previous findings unveiled that DAB2IP is down-regulated in high-grade PCa specimens and this novel tumor suppressor can block EMT leading to lymph node metastasis. It has recently been associated with the onset of cancer stem cell (CSC) that is considered as cancer initiating cell with a survival advantage during the course of cancer therapy. However, the mechanism of action is not fully characterized. Using microRNA microarray screening, we found microRNA-363 (miR363) is significantly down regulated in several DAB2IP knockdown (KD) prostate cells. In particular, miR363 is predominately expressed in normal prostate and belongs to the miR106a-363 cluster that is closely resembled to the oncogenic miR17-92 cluster in their seed sequence. It appears that DAB2IP significantly regulates the expression of a unique miR-363; the profile of miR-363 expression appears to be highly specific in normal prostate. The objective of this project is to delineate the functional links of miR-363 with the appearance of CSC and its clinical correlation in aggressive PCa.

15. SUBJECT TERMS

16. SECURITY CLASSIFICATION OF:			17. LIMITATION OF ABSTRACT	18. NUMBER OF PAGES	19a. NAME OF RESPONSIBLE PERSON
a. REPORT	b. ABSTRACT	c. THIS PAGE			USAMRMC
U	U	U	UU	11	19b. TELEPHONE NUMBER *(include area code)*

Table of Contents

INTRODUCTION

micoRNA (miR) is a large family of a short sequence of single-stranded noncoding RNAs, which has been shown to regulate approximate 60% protein-coding genes by post-transcriptional suppression, target mRNA degradation, or translational inhibition (1, 2). Until now, many miRs have been identified to be associated with different stages of tumor development. Based on their seed sequence of 2-7 nucleotides are grouped into different family for predicting the potential target gene(s), the function of miRs could be divided into onco-miR and tumor suppressor miR. However, only handful of them has been demonstrated experimentally.

DAB2IP (DOC-2/DAB2 interactive protein) was first identified as a new member of RAS-GTPase activating protein (RAS-GAP) family with growth inhibitory activity in prostate cancer (PCa). Loss of endogenous DAB2IP in PCa facilitates epithelial-to-mesenchymal transition (EMT) (3-5); tumor cells become highly metastatic in various lymph nodes from several orthotopic mouse models (6, 7). However, the underlying mechanism of DAB2IP in inhibiting EMT is not fully understood. Therefore, unveiling the mechanism of miR-mediated EMT signaling can provide more insights into the fundamental role of miRs contribute to tumorigenesis. Based on miR array screening, DAB2IP appears to regulate the expression of a unique miR-363. From our study, miR-363 is able to inhibit epithelial-to-mesenchymal transition (EMT) in PCa by targeting slug mRNA.

Unlike eukaryotic genes, several miRs are clustered together to generate a polycistronic primary transcript, which further complicates the regulatory scheme of miRNA biogenesis because each individual miR derived from one cluster may have different expression profile and functional role in any given cell or tissue. For example, miR-363 belongs to the polycistronic miR-106a-363 cluster containing six miRs (miR-106a, miR-18b, miR-20b, miR-19b-2, miR-92a-2 and miR-363). Unlike the other five miRs are closely resemble to the oncogenic miR-17-92 cluster in their seed sequence and functions (8), miR-363 has different functional role in suppressing tumor metastasis. In addition, the regulation of miR-363 is different from the rest of miRs from the same cluster. Thus, this project is to examine the regulation of miR363 in PCa and its correlation with PCa tumor grade.

BODY

During the third year we have unveiled the regulation of miR-363 by a unique RNA-binding protein and determine its expression status with PCa clinical specimens. The progress for each aim is summarized as follows:

Study the regulation of miR363 gene expression by DAB2IP.
RNA immunoprecipitation (RIP) and mass spectrophotometry were performed to identify protein molecules associated with the processing machinery of pre-miR-363, interferon-induced tetratricopeptide repeat protein (9, 10), IFIT5, was identified as a potential

candidate. The specific association between IFIT5 and pre-miR-363 was further verified in western blot analysis, in which we found an increased association of IFIT5 with pre-miR-363 in RWPE1-KD cells, compared to RWPE1-Con cells (Fig. 1A). This inverse correlation between DAB2IP and IFIT5 was further confirmed by a dose-dependent reduction of IFIT5 by DAB2IP overexpression in both LAPC4-KD (Fig. 1B) and C4-2Neo cell lines (Fig. 1C).

In order to examine whether IFIT5 plays a critical role in DAB2IP-mediated miR-363 upregulation, we overexpressed IFIT5 in DAB2IP-positive cells (LAPC4-Con, C4-2D2 and RWPE1-Con) using pcDNA3.1-3XFLAG-IFIT5 plasmid, and tested the expression level of miRNA components derived from the miR-106a-363 cluster using quantitative RT-PCR. In LAPC4-Con cells, the qRT-PCR screening showed that IFIT5 induced slightly upregulation of pre-miR-18b and pre-miR-20b, but not pre-miR-19b, pre-miR-92a-2 and pre-miR-363, compared to empty vector control. In contrast, the mature miR-363 was significantly downregulated, while other miRNA components remained relatively no change in response to IFIT5 induction in LAPC4-Con cells (Fig. 1D). On the other hand, we observed both pre-miR-363 and mature miR-363 are significantly downregulated by IFIT5 in C4-2D2 cell line, while other miRNA components showed relatively mild change in their precursor and mature level (Fig. 1E). Similar to LAPC4-Con cell, IFIT5 induced a significant upregulation of pre-miR-18b and pre-miR-20b in RWPE1-Con cells. On the contrary, pre-miR-19b, pre-miR-92a-2 and pre-miR-363 showed only slightly downregulation by IFIT5 induction (Fig. 1F). On the other hand, the mature miR-18b, miR-20b, miR-19b and miR-92-2 in RWPE1-Con cells were all upregulated at various levels, while mature miR-363 expression was significantly reduced by IFIT5 induction (Fig. 1F). Overall, in contrast to other components in the miR-106a-363 cluster, miR-363 exhibited a unique expression pattern in response to IFIT5 induction among three DAB2IP-positive cell lines (LAPC4-Con, C4-2D2 and RWPE1-Con). On the contrary, miR-18b, miR-20b, miR-19b and miR-92a-2 maintained relatively mild or no change at their precursor and mature level (Fig. 1G). Similar to LAPC4-KD cells, we also observed a dramatic elevation of mature miR-363 in C4-2Neo cells (Fig. 2H), RWPE1-KD (Fig. 1I). This finding demonstrates that IFIT5 can specifically interfere with miR-363 processing from precursor to mature form.

In contrast to the significant increase of pre-miR-363 fragments, the degradation rate of pre-miR-92a-2 was relatively mild (Fig. 2A), suggesting that pre-miR-363 may be a unique substrate for IFIT5-mediated RNase activity. By comparing the precursor structure between pre-miR-92a-2 and pre-miR-363, we found pre-miR-92a-2 has a sealed double-strand at the end of its precursor stem, whereas pre-miR-363 has a single nucleotide (U) overhang at its 5'end. Therefore, we designed a mutant form of pre-miR-363 with either a single strand of six nucleotides overhang at its 5'end (SSMut pre-miR-363), or a sealed double strand between its 5'and 3'end (DSMut pre-miR-363) (Fig. 2B). The corresponding sequence designated for mutation in the precursor structure does not cover the leading or passenger strand of mature miR-363. Both SSMut and DSMut pre-miR-363 sequences were either cloned into the pCMV-miRNA vector for expression and functional analysis, or attached to a T7 promoter to generate the DNA template for *in vitro* transcription of both mutant pre-miR-363 RNA molecules. In order to investigate whether the 5'end region of precursor structure has any effect on the maturation process of miR-363, LAPC4-KD cells were transfected with pCMV-miRNA plasmids carrying

native, SSMut or DSMut pre-miR-363, and the expression level of mature miR-363 was examined. The transfection efficiency of native and mutant pre-miR-363 plasmids were relatively equal, based on a relatively equivalent expression of primary miR-363 transcript. On the other hand, compared to the miR-363 derived from native form, the expression level of SSMut-derived mature miR-363 was significantly lower, while DSMut-derived mature miR-363 was highly upregulated in LAPC4-KD cells. The similar expression pattern of native, SSMut and DSMut pre-miR-363 plasmids were also seen at the precursor level with a less significant fold induction (Fig. 2C). This evidence indicates that the 5'end region of pre-miR-363 structure may determine the efficacy of miR-363 maturation. Given that IFIT5 exhibits a unique impact on miR-363 maturation and enhances RNA degradation of pre-miR-363 *in vitro*, we asked whether the 5'end region of pre-miR-363 determines the specific regulation by IFIT5. We incubated native, SSMut and DSMut pre-miR-363 RNA molecules with IFIT5 protein and examined the degradation rate of each precursor. Compared to the degradation rate of native pre-miR-363, the fragmented form of SSMut pre-miR-363 increased significantly following the incubation time course, while DSMut pre-miR-363 showed a relatively mild degradation rate (Fig. 2D). Notably, the degradation rate of each precursor is inversely correlated with the expression level of its mature form in LAPC4-KD cells (Fig. 3C), indicating the the turnover miR-363 is partly attributed to IFIT5-mediated RNA degradation of pre-miR-363. To examine whether the 5'end region of pre-miR-363 is critical for the IFIT5-mediated specific turnover of miR-363, we transfected LAPC4-KD cells with both SSMut and DSMut pre-miR-363 plasmids in the absence of IFIT5. We observed a dose-dependent recovery of SSMut-derived mature miR-363 expression following the knockdown of IFIT5. While miR-363 derived from DSMut pre-miR-363 at significantly higher level did not affected by the absence of IFIT5 (Fig. 2E). Moreover, to confirm the specific interaction between the 5'end region of pre-miR-363 and IFIT5 protein, we performed RIP using *in vitro* transcribed SSMut and DSMut pre-miR-363 RNA molecules to pull down protein components in LAPC4-KD cell, which has abundant endogenous IFIT5 protein. We observed a significantly higher association between IFIT5 and SSMut pre-miR-363, while DSMut pre-miR-363 was merely found to interact with any IFIT5 protein (Fig. 2F). This evidence indicated IFIT5 has a specific RNA-recognition preference for miRNA molecule with single-stranded overhang structure. Overall, these observations revealed that IFIT5 mediates pre-miR-363 degradation and hence down regulates mature miR-363 expression via targeting the 5'end region in the precursor miRNA structure.

Study the correlation of DAB2IP and miR363 in PCa progression.

We screened the expression level of IFIT5 mRNA using human PCa specimens and observed a trend of increasing IFIT5 expression in a more malignant PCa tissue, compared to benign tissue and lower grade (G6) PCa (Fig. 3A). On the other hand, we also analyze the expression level of mature miR-363 as well as two other components derived from the same miR-106a-363 cluster. Compared between the benign and a lower grade of PCa tissues (G6), no significant difference was found in miR-363 expression level. In contrast, a significant upregulation miR-19b was observed in an early disease stage of G6, throughout the malignant PCa tumors (G7, G8 and G9) (Fig. 3B). Meanwhile, a trend of down-regulation was observed in both miR-363 and miR-19b throughout the malignant PCa tumors from G6 to G9 stage. However, expression of miR-

363 decreased more dramatically in high grade PCa tumor (G8 and G9), compared to miR-19b (Fig. 3B). On the other hand, we also observed a significant elevation of miR-92a-2 in malignant PCa tumor at the stage of G6, compared to benign tissues. However, the level of miR-92a-2 expression in the different grade of PCa tumors do not vary much as that of miR-363 levels (Fig. 3B).

Knowing that IFIT5 mRNA expression is significantly upregulated in malignant prostate tissues (Fig. 3A), while miR-363 showed a trend of downregulation in more aggressive PCa specimens (Fig. 3B). Here we examined the clinical correlation between IFIT5 and miR-363 expression in PCa. Notably, an inverse while significant correlation was demonstrated between IFIT5 mRNA and miR-363 expression level among both benign and malignant prostate tissues (Fig. 3C). Based on the TGCA data set, we found a positive while significant correlation between IFIT5 and XRN1 (a RNase) (Fig. 3D). Overall, the clinical correlation between IFIT5, XRN1 and miR-363 suggests the lost of miR-363 in aggressive PCa tumors may partly attribute to the upregulation of both IFIT5 and XRN1 during the disease progression of PCa. Altogether, in this study we demonstrated a unique expression of miR-363 from an oncogenic miR-106a-363 cluster is processed through special machinery different from other miRNA components. Both IFIT5 and XRN1 proteins are involved in this unique processing machinery via interaction with pre-miR-363, which lead to specific turnover of pre-miR-363 molecule.

KEY RESEARCH ACCOMPLISHMENTS

- IFIT5 complex can specifically degrade mature miR-363 in PCa cells.
- IFIT5-XRN1 complex represents a novel machinery for miR-363 turnover.
- Loss of miR363 expression is correlated with PCa development.
- Increased IFIT5 expression is correlated with PCa development.
- A positive correlation between IFIT3 and XRN1 expression was observed in clinical PCa database.

REPORTABLE OUTCOMES

Lo, U., Yang, D., Hsieh, J.T. (2013) The role of microRNAs in prostate cancer progression. Trans. Androl. Urol., 2: 228-241.

CONCLUSION

Interferon-induced tetratricopeptide repeat (IFIT) protein family is first identified as viral RNAs biding protein that is a part of antiviral defense mechanisms by reducing virus replication or disrupt protein–protein interactions in host translation-initiation machinery. Among IFIT orthologs, IFIT1, IFIT2 and IFIT3 form a complex through its tetratricopeptide repeats (TPR). On the contrary, IFIT5 acts solely as a monomer and binds directly to RNA molecules via its convoluted RNA-binding cleft. In a recent study, IFIT5 has been shown to directly bind to endogenous cellular RNA with a 5'-end phosphate cap, including transfer RNA (tRNA), which partially shared a structural similarity with the precursor form of small RNAs such as small hairpin RNA (shRNA) and miRs. We have demonstrated the first time that IFIT5 is able to specifically

recognize a unique structure in the precursor miR-363 and recruit XRN1 to degrade miR363. We have also shown that the significant elevation of IFIT5 is detected in several PCa cells undergone EMT leading to highly metastatic potential. In addition, the expression level of IFIT5 is correlated with that of miR-363 in PCa specimens. Taken together, this study unveils a new mechanism for the stability and the functional role of a unique miR distinct from other cluster member in PCa cells

REFERENCES

1. Aalto AP, Pasquinelli AE. (2012) Small non-coding RNAs mount a silent revolution in gene expression. Current Opinion In Cell Biol. 24:333-340.
2. Schickel R, Boyerinas B, Park SM, Peter ME. (2008) MicroRNAs: key players in the immune system, differentiation, tumorigenesis and cell death. Oncogene 27:5959-5974.
3. Thiery JP (2002) Epithelial-mesenchymal transitions in tumour progression. Nat. Rev. Cancer 2**:**442-454.
4. Yang J, Weinberg RA (2008) Epithelial-mesenchymal transition: at the crossroads of development and tumor metastasis. Dev. Cell 14:818-829.
5. Mani SA, et al. (2008) The epithelial-mesenchymal transition generates cells with properties of stem cells. Cell 133:704-715.
6. Xie, D, et al. (2009) DAB2IP/AIP1, a novel tumor suppressor, coordinates both PI3K-Akt and ASK1 pathways. Proc. Natl. Acad. Sci., USA 106:19878-19883.
7. Xie, D, et al. (2010) The role of DAB2IP in modulating epithelial-to-mesenchymal transition and prostate cancer metastasis. Proc. Natl. Acad. Sci., USA 107:2485-2490.
8. Landais S, et al. (2007) Oncogenic potential of the miR-106-363 cluster and its implication in human T-cell leukemia. Cancer Res. 67:5699-5707.
9. Abbas YM, et al. (2013) Structural basis for viral 5'-PPP-RNA recognition by human IFIT proteins. Nature 494:60-64.
10. Katibah GE, et al. (2013) tRNA binding, structure, and localization of the human interferon-induced protein IFIT5. Molecular Cell 49:743-750.

Appendices

Figure 1 The specific role of IFIT5 in regulating the level of mature miR-363 from other members in the miR-106a-363 cluster. (A) RNA immunoprecipitation assay identified association between precursor-miR-363 and IFIT5 protein in in DAB2IP-positive and –negative sublines including LAPC4, RWPE1 and C4-2 cell lines. (B) Reduction of IFIT5 protein level in DAB2IP-overexpressed LAPC4-KD cells. (C) Reduction of IFIT5 protein level in DAB2IP-overexpressed C4-2Neo cells. (D-F) Expression level of precursor and mature miRNAs (miR-18b, miR-20b, miR-19b, miR-92a-2 and miR-363) in IFIT5-overexpressed (IFIT5) LAPC4-Con, C4-2D2 and RWPE1-Con cells, compared to empty vector control (Vec). (G-I) Expression level of precursor and mature miRNAs (miR-18b, miR-20b, miR-19b, miR-92a-2 and miR-363) in IFIT5-knockdown (siRNA-IFIT5) LAPC4-KD, C4-2Neo and RWPE1-KD cells ,compared to control siRNA (siRNA-Con).

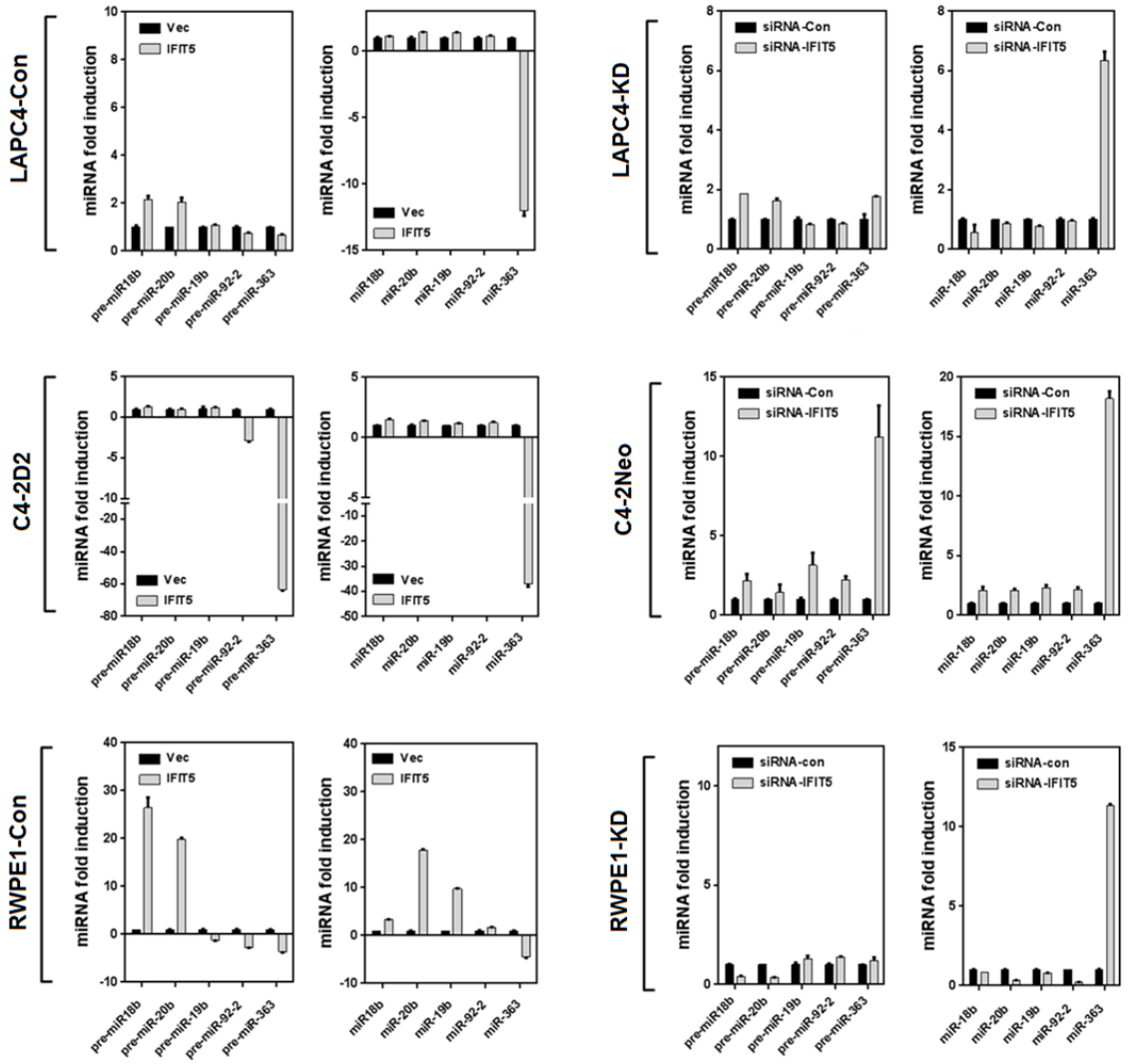

Figure 2 IFIT5-mediated precursor miR-363 degradation *in vitro*. (A) Time-dependent relative fold change of pre-miR-92-2 and pre-miR-363 fragments after incubation with IFIT5 protein at 37°C. (*P<0.05) (B) Mutation of nucleotides (red box) for generating 5'-end single stranded pre-miR-363 (SSMut pre-miR-363) and 5'-end double stranded pre-miR-363 (DSMut pre-miR-363). Both mature miR-363 and miR-363* sequence are labeled in pink. (C) Expression level of primary, precursor and mature miR-363 in LAPC4-KD cells transfected with native, SSMut and DSMut pre-miR-363 plasmids for 24 hours, compared with empty vector control (Vec). (D) Time-dependent relative fold change of native, SSMut and DSMut pre-miR-363 fragments after incubation with IFIT5 protein at 37°C. (*p<0.05) (E) IFIT5 knockdown induced expression of mature miR-363 derived from SSMut and DSMut pre-miR-363 plasmids (*p<0.05). (F) RNA pull down assay identified the association between IFIT5 protein and SSMut or DSMut pre-miR-363.

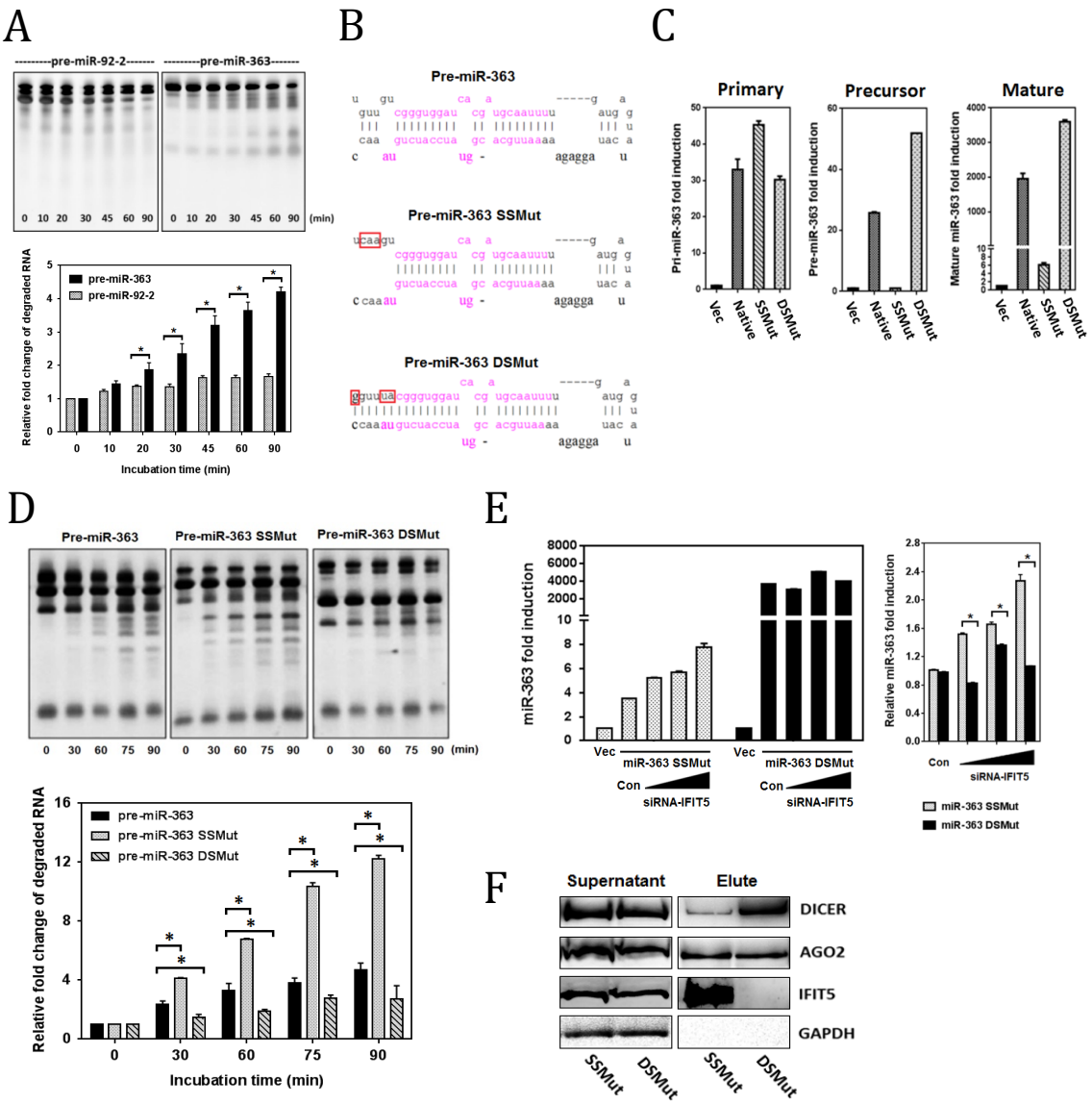

Figure 3 Clinical correlation of IFIT5 expression with PCa (A) IFIT5 mRNA expression in human PCa specimen at different disease stage. (B) Expression of miR-363, miR-19b and miR-92a-2 in human PCa specimen at different disease stage. (C) Clinical correlation between IFIT5 and miR-363 in human PCa specimen. (D) Clinical correlation between IFIT5 and XRN1 in PCa (*p<0.05, **p<0.001, ***p<0.0001 indicate statistic significance)